Environmental Pollution 159 (2011) 1673–1681

Contents lists available at ScienceDirect

Environmental Pollution

journal homepage: www.elsevier.com/locate/envpol

Biomagnetic monitoring of industry-derived particulate pollution

R. Hansard [a,*], B.A. Maher [a], R. Kinnersley [b]

[a] Centre for Environmental Magnetism and Palaeomagnetism, Lancaster Environment Centre, University of Lancaster, Lancaster LA1 4YQ, UK
[b] Evidence Directorate, Environment Agency, Olton Court, 10 Warwick Road, Olton, Solihull B92 7HX, UK

Biomagnetic techniques are used for quantitative mapping of particulate pollution at uniquely high spatial resolution and to distinguish between differently-sourced PM_{10}.

ARTICLE INFO

Article history:
Received 11 November 2010
Received in revised form
28 January 2011
Accepted 26 February 2011

Keywords:
Magnetic biomonitoring
Deposition velocity
PM_{10} monitoring
Tree leaves
Source attribution

ABSTRACT

Clear association exists between ambient PM_{10} concentrations and adverse health outcomes. However, determination of the strength of associations between exposure and illness is limited by low spatial-resolution of particulate concentration measurements. Conventional fixed monitoring stations provide high temporal-resolution data, but cannot capture fine-scale spatial variations. Here we examine the utility of biomagnetic monitoring for spatial mapping of PM_{10} concentrations around a major industrial site. We combine leaf magnetic measurements with co-located PM_{10} measurements to achieve inter-calibration. Comparison of the leaf-calculated and measured PM_{10} concentrations with PM_{10} predictions from a widely-used atmospheric dispersion model indicates that modelling of stack emissions alone substantially under-predicts ambient PM_{10} concentrations in parts of the study area. Some of this discrepancy might be attributable to fugitive emissions from the industrial site. The composition of the magnetic particulates from vehicle and industry-derived sources differ, indicating the potential of magnetic techniques for source attribution.

1. Introduction

In recent years, identification of the adverse health effects associated with exposure to particles smaller than 10 μm aerodynamic diameter (PM_{10}), particularly those smaller than 2.5 μm in diameter ($PM_{2.5}$), has been an active and growing research area. Short-term (<1 h) exposure to peak levels of PM_{10} has been strongly associated with adverse cardiovascular and respiratory health impacts (e.g. Curtis et al., 2006; Schwarze et al., 2006). However, epidemiological and toxicological studies also indicate that longer-term cumulative exposure to relatively small increases ($<10\ \mu g\ m^{-3}$) in ambient PM_{10} and $PM_{2.5}$ concentrations impact adversely on human health (e.g. COMEAP, 2009). Additionally, Pope et al. (2009) have shown a marked improvement in health outcomes in response to programmes of active reduction of ambient particulate pollution concentrations. Their findings suggest that reductions in ambient particulate pollution concentrations of just $10\ \mu g\ m^{-3}$ are associated with increased life expectancy, independent of socioeconomic, demographic or lifestyle (e.g. smoking habits) factors.

However, the specific causal links between the degree of exposure and the likelihood/severity of adverse health impacts within a population remain uncertain, and calculated risk estimates also differ between studies (e.g. Schwarze et al., 2006). This may be due at least in part to the reliance of many epidemiological studies on exposure data from relatively low spatial-resolution networks of monitoring stations (e.g. up to 5 miles from residences; e.g. Karr et al., 2006; Woodruff et al., 2006). Such coarse-scale data are a limiting factor in determining dose response relationships at an individual rather than population level, due to finer-scale variations in particulate pollution concentration and/or size across the urban environment (e.g. Brook et al., 2004; Monn, 2001), depending on particle source.

A global increase in implementation of mitigation techniques (e.g. Balat, 2008; Minguillón et al., 2009) has led to a decline in emissions of industrially-sourced particulate matter (e.g. EEA, 2008). However, despite decreasing pollution emissions from industrial point sources, monitoring shows that industry continues to impact on local and regional particle concentrations at a range of distances from the source (e.g. Sharma and Tripathi, 2008; Wang et al., 2010). Our ability to fully understand and quantify, and hence manage down, such contributions is currently limited by the scarcity of monitoring data that are generally available. While temporal resolution is high, spatial coverage tends to be poor,

* Corresponding author.
E-mail address: r.hansard@lancaster.ac.uk (R. Hansard).

0269-7491/$ – see front matter © 2011 Elsevier Ltd. All rights reserved.
doi:10.1016/j.envpol.2011.02.039

limiting our ability to resolve between, for example, multiple sites of emission.

In an effort to address the low spatial density of conventional fixed monitoring stations, PM_{10} surfaces have been modelled. Atmospheric dispersion modelling systems such as ADMS 4.1 (CERC Ltd., Cambridge, UK; CERC, 2010) or AERMOD (US Environmental Protection Agency; U.S. EPA, 2010a) are widely used to model emissions from industrial pollution sources for regulatory purposes. Dispersion models use meteorological data, stack height and diameter, in addition to estimates of emission quantities, temperature and exit velocity, to model the dispersion of industry-derived particulate emissions. However, validation data at high spatial resolution are sparse, and quality of model parameters can be limited; for example, emission data are often approximated from diurnally-trended monthly fuel usage, while data taken from the nearest meteorological station to the study area may not be fully representative due to local-scale variability. Additionally, detailed knowledge of all emissions (especially on complex sites) and the effects of varying terrain on PM dispersion and deposition is limited at present, resulting in uncertainty in modelled results (e.g. Parker and Kinnersley, 2004).

There is thus a need for high spatial-resolution particulate pollution monitoring techniques which are able to capture local variation in pollutant concentration.

Biomagnetic monitoring, using tree leaves as sampling surfaces, can generate high spatial-resolution PM_{10} proxy data. Whilst urban anthropogenic particulates may consist of a complex mixture of organic and inorganic components, they almost invariably contain magnetic particles, which derive from iron impurities in the fuel. Upon combustion, a non-volatile magnetic residue is formed, often a mixture of ferrimagnetic (magnetite/maghemite-like) and imperfectly antiferromagnetic (haematite-like) iron oxides. In urban particulates, a strong correlation has been observed between magnetic susceptibility/remanence and PM_{10} concentrations (e.g. Morris et al., 1995; Muxworthy et al., 2003; Sagnotti et al., 2006; Szönyi et al., 2008), as a proxy for particulate pollution concentrations. Magnetic techniques are sensitive and rapid (e.g. Matzka and Maher, 1999; Muxworthy et al., 2003; Maher et al., 2008; Szönyi et al., 2008). Tree leaves provide particularly good sampling surfaces as they are already prevalent throughout the urban environment and require no power source or protection from vandalism. Whilst this approach is limited, for deciduous species, to the in-leaf season (i.e. $\sim$ 8 months p.a.), the spatial resolution of PM_{10} mapping enabled by this technique represents a step change improvement in current data availability.

This study focuses on deciduous tree leaves, reflecting both species availability in the study area (S. England) and previously established species inter-calibration data (Mitchell et al., 2010). In order to identify ambient particulate pollution levels, it is necessary to use leaves from tree species which reach dynamic equilibrium with ambient PM_{10} concentrations rapidly, i.e. by surface capture of particles (Mitchell et al., 2010) rather than internal uptake of particles into the leaf structure (e.g. Lehndorff et al., 2006). Leaves from the deciduous species used here (Methods section below) have been found to reach magnetic dynamic equilibrium (e.g. Chamberlain and Chadwick, 1972) at the roadside after $\sim$ 6 days (Mitchell et al., 2010) compared to an equilibration time of >2 years for evergreen species (e.g. Lehndorff et al., 2006).

Variations in leaf shape and surface morphologies are the probable cause of variations in particulate dry deposition velocities to the leaf surface of different tree species. Deposition velocity of particles to ridged/hairy leaf surfaces is likely to be much greater than to smooth/waxy leaves. Consistent deposition velocities have been reported for several tree species (e.g. Freer-Smith et al., 2005; Mitchell et al., 2010). Magnetic measurements of leaves from several deciduous species can thus be inter-calibrated (Mitchell et al., 2010), optimising sampling density and resultant spatial resolution of the proxy PM_{10} data.

Previous work has shown that magnetic biomonitoring can be a robust, quantitative technique for identifying ambient concentrations of anthropogenic PM_{10}; strong correlation has been demonstrated between leaf saturation remanent magnetisation (SIRM) and/or magnetic susceptibility (χ) values and the amount of combustion- and/or abrasion-derived pollution particles on the leaf surface (e.g. Halsall et al., 2008; Maher et al., 2008; Szönyi et al., 2008). Correlations between magnetic parameters and toxic metals, such as lead, zinc and iron, have also been identified (e.g. Lu and Bai, 2006; Maher et al., 2008; Morton-Bermea et al., 2009).

Here, we report a biomagnetic study which monitored particulate pollution around a large combustion plant in the U.K.. The site has 1 chimney stack, $\sim$200 metres tall, with annual mean emission rates $\sim$ 6 m s^{-1} (range = 0.1–11.89 m s^{-1}). First, we examine leaf-magnetic data, combined with co-located ambient PM_{10} concentrations (from SidePak AM510 personal aerosol monitors), in order to assess how representative leaf magnetic values are of ambient particulate concentrations. We then use the biomagnetic data to quantify PM_{10} concentrations at high spatial resolution, and compare the leaf-derived and measured PM_{10} concentrations with those predicted by a conventional dispersion model. Finally, we briefly compare the magnetic characteristics of vehicle- and industry-derived pollutant particles from sites in the U.K.

2. Methods

A pilot biomagnetic study was carried out in 2006, with leaves sampled from 12 sites along north and east transects (9 km N and 11 km E) originating at the elevated stack of a large combustion plant located in England. Subsequently, leaves from 52 sites around the plant were sampled at monthly intervals from May to September, 2008, with an additional campaign in September 2009 (Fig. 1). Rainfall and transient inputs of relatively 'non'-magnetic PM_{10} from distal sources (e.g. tropical/sub-tropical dust storms) can affect the attainment of dynamic equilibrium between leaf surface and ambient PM_{10} concentrations (Sagnotti et al., 2006). Available fixed monitoring station data indicate that the sample locations used in this study were not influenced by transient peaks in long range transported particulates. To minimise any local meteorological effects, sampling was always done within two consecutive, rain-free days.

With the exception of the 2006 pilot study (when both high tree and low shrub canopy samples were collected), leaf samples were collected at 1.5–2 m height from trees located at >30 m from any road, in order to minimise the contribution from immediately adjacent sources, such as traffic (e.g. Hoffmann et al., 1999; Szönyi et al., 2008). To obtain data at highest possible spatial resolution, using the previously-established inter-species calibration (Mitchell et al., 2010), the following tree species were sampled: birch (*Betula pendula*), beech (*Fagus sylvatica*), lime (*Tilia platyphyllos*), field maple (*Acer campestre*), ash (*Fraxinus excelsior*), sycamore (*Acer pseudoplatanus*), elder (*Sambucus nigra*), elm (*Ulmus procera*), and willow (*Salix alba*).

All leaf samples were refrigerated at 5 °C before being taken to the Centre for Environmental Magnetism and Palaeomagnetism (CEMP) at Lancaster University for magnetic analysis using the protocol outlined in Mitchell and Maher (2009). Appendix 1 provides a short explanation of the magnetic parameters used.

Co-located PM_{10} concentration data were collected from a subset of sites (37) over the whole sample area during the September 2009 campaign, using handheld SidePak AM_{510} personal aerosol monitors.

3. Results

3.1. Leaf magnetic values and particulate pollution

In the initial pilot study (2006), leaf magnetic enrichment ratios (ER) were measured for leaves from 12 locations along north and east sampling transects (Fig. 2). Leaves were collected from both high (>1.5 m) and low (<0.5 m) canopy vegetation. For calculation of the ERs, all values were divided by a 2006 background (leaf area-normalised) SIRM value (measured >10 km from the source) of 3×10^{-6} A; this value is consistent with measured background

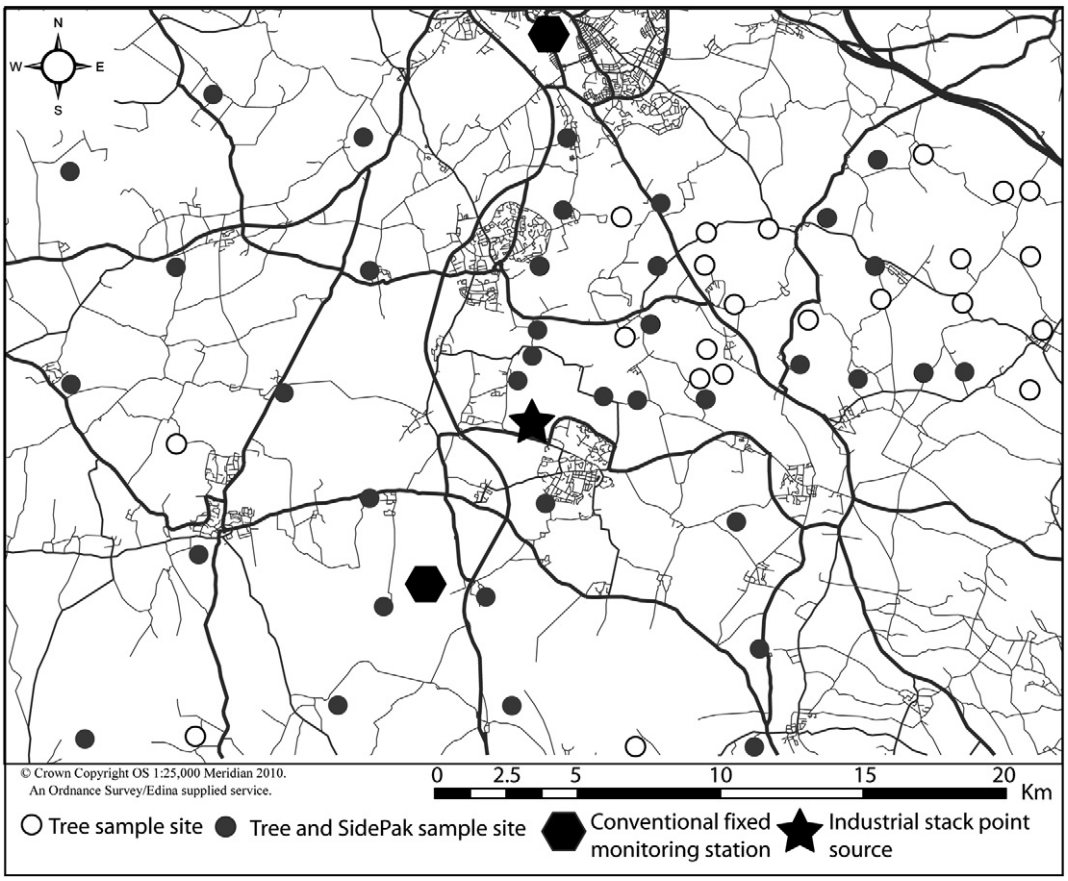

Fig. 1. Map showing the major industrial point source, conventional fixed monitoring stations, road network (motorway and A-roads indicated in bold), tree sampling sites (all months) and SidePak ambient PM_{10} monitoring sites (September 2009).

SIRM values in Lancashire and East Anglia, UK (Mitchell and Maher, 2009; Maher et al., 2008). High- and low-level leaf samples exhibit different trends with distance from the stack point source (Fig. 2). Close to the source, low level foliage (nettles) exhibited high ER values (up to 60), which rapidly decreased within 2 km in both directions. Higher level foliage (sycamore) displayed initially low leaf SIRM ERs (10–30), which increased to a peak (30–50) at about 2 km from the source, decreasing beyond this point. Brambles generally followed the same trend as the trees along both transects (with one anomalously low value ~ 2 km north of the source).

Subsequently, sampling of tree canopy leaves (~ 1.5–2 m height) was carried out at monthly intervals (summer 2008, summer 2009). These monthly samples revealed consistent peaks in leaf SIRM values at <2 and ~5–10 km from the point source (Appendix 2). Fig. 3 shows the distribution of leaf SIRM values around the stack point source, for September, 2008. Maximum (species-normalised) leaf SIRM values in September 2008, measured within 2 km of the source, were ~ 6 × higher than the background values (12.6×10^{-6} A compared with 2.1×10^{-6} A). The highest leaf values occurred NE and SW of the point source. There is no evidence of progressive increase in leaf SIRM values with time. For example, leaf SIRMs in August 2008 were lower than those obtained in the preceding June and July 2008, whilst values increased again in September 2008. Nor is there any evidence of direct influence of local, traffic-derived pollution; the spatial pattern of leaf SIRMs varies independently of the sample distance from the road networks (multivariate regression analysis; $t = -0.586$, $p = 0.56$, $n = 168$; Fig. 3a). To assess the reliability of the tree leaves as PM collectors, ambient PM_{10} concentrations were measured at a subset of the sampled tree locations. In September 2009, 37 samples were collected using a handheld SidePak AM510 personal aerosol monitor (5-minute sample time). The measured ambient PM_{10} concentrations around the point source ranged from 2 to 35 $\mu g\, m^{-3}$ (Fig. 3b), with highest concentrations observed in the direction of the prevailing wind, at distances < 2 and ~ 5–10 km from the point source. The co-located ambient PM_{10} values display correlation with the leaf SIRM values (September, 2009) ($R^2 = 0.71$, $p = 0.01$, $n = 37$, Fig. 4).

The strong correlation identified between leaf SIRM values and ambient particulate concentrations indicates that the average wind pattern over the leaf equilibration period was similar to the wind pattern (speed and direction) on the days of active air sampling. In September 2009, the SW component was greater than the NE component, and the pattern was dominated by higher wind speeds ($5\ m\ s^{-1} < u < 16\ m\ s^{-1}$; Fig. 4c).

We can use deposition velocity

$$(mV_d)\ \text{calculations}\ (mV_d) = \text{flux/concentration} \quad (1)$$

where flux = $SIRM_{leaf}/m^2 s$ and concentration = $SIRM_{filter}/m^3$ based on time series experiments with controlled leaf exposure periods (Hazelrigg, UK data; Fig. 5) to estimate the time period of leaf exposure prior to equilibration with ambient PM_{10} concentrations here.

To attain dynamic equilibrium (e.g. Chamberlain and Chadwick, 1972) around this industrial source, the calculated exposure time is ~20 days. However, this is a minimum value, as it does not account for loss during rain episodes or periods with lower than average

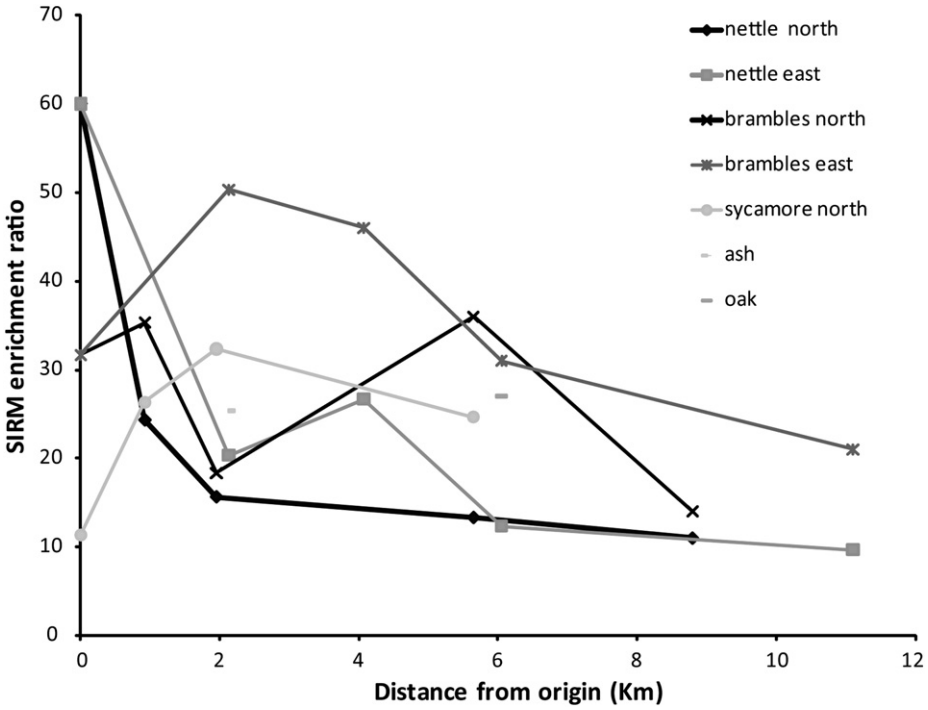

Fig. 2. Pilot study results showing trends in leaf SIRM enrichment ratios with distance from the stack point source.

ambient PM_{10} concentrations. Starting with 20 days prior to the leaf sampling and progressively increasing the dataset in 24-hour timeslots, the wind patterns were assessed for similarity with the wind pattern when active air sampling took place. Strong similarity is identified between the wind patterns on the days of active air sampling and the average wind patterns by inclusion of meteorological data up to 32 days prior to leaf sampling (Fig. 4b and c).

It is useful to compare the correlation observed at a predominantly traffic-influenced site between ambient PM_{10} concentrations and leaf SIRM values with that seen in the present study, where samples have been taken at a distance from roads but potentially impacted by the industrial site and its large combustion plant. While strong correlations are observed between leaf magnetic values and ambient concentrations in both contexts, the correlations differ; the traffic-influenced leaf SIRM values (Hazelrigg, U.K.) are up to three times greater than those measured here (Fig. 5). This might be explained by a lower mean deposition velocity around this industrial site, inferring a difference in the magnetic particle size fraction. However, it might also be explained by a difference in the composition of the magnetic particulates predominant in the traffic- and the industry-derived emissions.

3.2. Magnetic mineralogy and particle characteristics

The three main factors contributing to the measured leaf magnetic properties are magnetic mineralogy, concentration and magnetic grain size. The leaves around this U.K. stack point source acquired some magnetic remanence at low applied fields, indicating the presence of at least some magnetically soft material, such as magnetite; ~15% of the total room temperature remanence was acquired below 20 mT, ~ 40% by 50 mT and ~ 60% by 100 mT. However, between 5 and 15% of the SIRM was acquired between 100 and 300 mT, and up to 15% acquired at high magnetic fields, i.e. above 300 mT (% HIRM). Additionally, the samples retain 25–50% of their HIRM upon AF demagnetisation at 100 mT. Such "hard" magnetic behaviour is characteristic of haematite, of ~0.2 μm grain size (Maher et al., 2004). Notably, the 15 samples collected within ~2 km of the industrial site were all magnetically distinct from those collected further away; in all months, samples local to the source were characterised by lower % HIRM (<5%) and χ_{ARM}/SIRM ($<13 \times 10^{-5}$ A^{-1}) values than other, more distal samples in the study area.

Because haematite has much lower magnetisation than magnetite, it must be present in high concentrations, relative to magnetite, in order to contribute the HIRMs measured here. The magnetite: haematite ratio for these leaf samples is estimated at ~1:32 (i.e. based on their HIRM and 'S' ratios (Table 1; Frank and Nowaczyk, 2008). In absolute terms, comparison of magnetic properties (IRM_{20}, HIRM) of synthetic ferrimagnets with those of roadside samples (Lancaster, UK; Mitchell and Maher, 2009) indicates the presence of approximately equal concentrations of haematite and magnetite (~0.2%). Conversely, the samples from this industrial point source study indicate the presence of ~ 0.01% haematite, but only ~ 0.0001% magnetite. Thus, compared with strongly vehicle-influenced PM_{10}, the ambient particulate emissions around the area in this study contain much greater haematite concentrations. This difference of ~2 orders of magnitude in the haematite:magnetite ratio can thus account for the different leaf/PM_{10} correlations shown in Fig. 5.

Taking into account these relatively high haematite concentrations in the industry-influenced pollutants, leaf-measured χ_{ARM}/SIRM values may be up to 75% lower than those expected from pure magnetite (Frank and Nowaczyk, 2008; Fig. 6). Corrected χ_{ARM}/SIRM values indicate, for the magnetite component of the leaf particles, a dominant magnetic grain size of ~0.1–1 μm (Maher, 1988).

3.3. Comparison of leaf-calculated PM_{10} with modelled PM_{10} concentrations

Given the strong correlation between the SIRMs of tree leaves and independently-measured, co-located ambient PM_{10} concentrations,

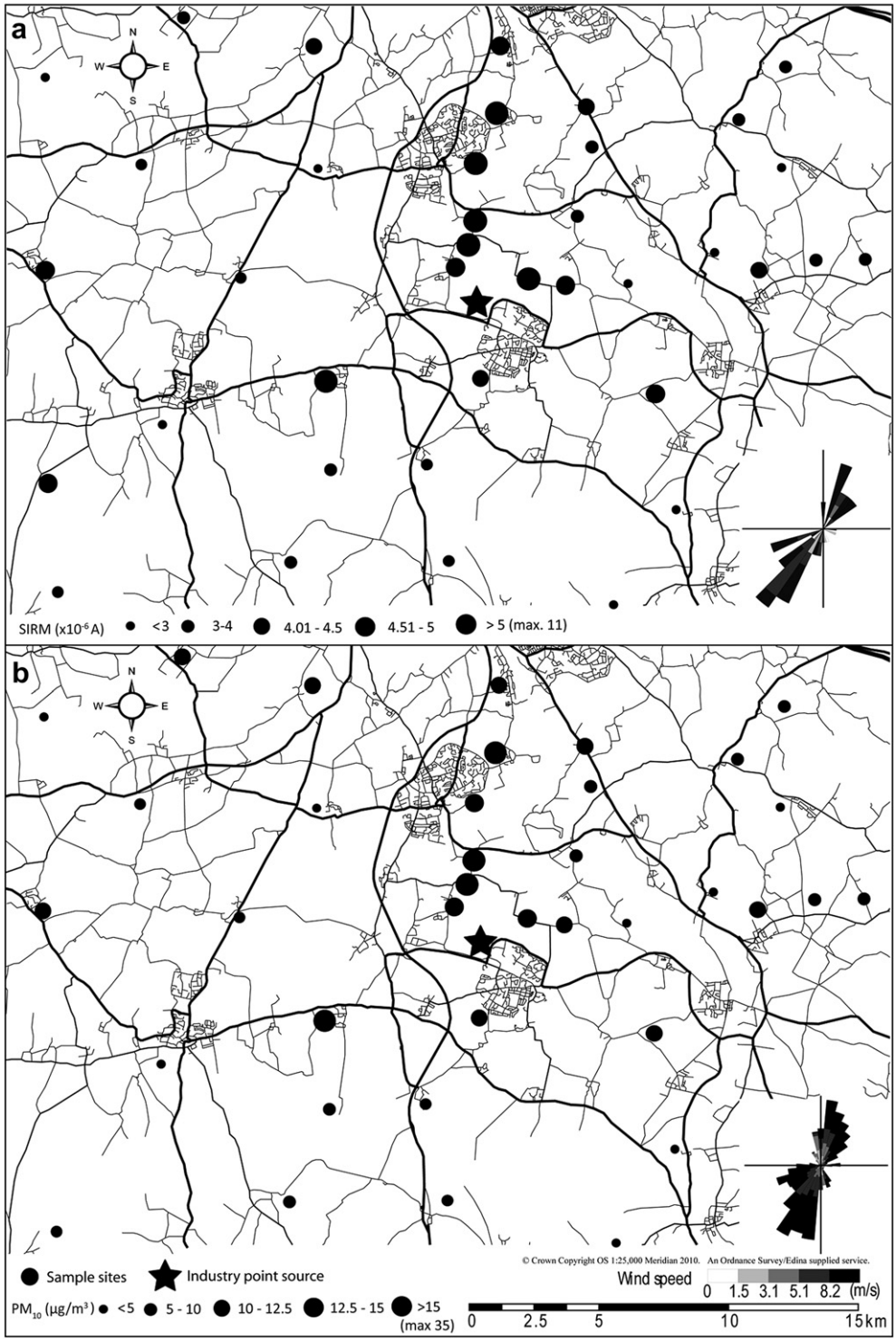

Fig. 3. (a) species-normalised (Mitchell et al., 2010) leaf magnetic values and (b) conventionally-measured PM_{10} concentrations for September 2009. Local wind speed and direction for 32 days and 2 days prior to sampling shown bottom right of figures a & b, respectively.

leaf SIRMs can be used as a robust, quantitative proxy for particulate pollution around this potential industrial source of particulate pollution. Leaf-calculated PM_{10} concentrations around this industrial site range from 6 $\mu g/m^3$ to 41.3 $\mu g/m^3$, with the highest values located ~2 and ~4 km north of the stack (Fig. 7a). Interpolating between the leaf-calculated PM_{10} values (using inverse distance weighted (IDW) interpolation) produces a PM_{10} concentration of 17 $\mu g/m^3$ at the location of, and in agreement with, the single conventional fixed monitoring station location within the study area (15 $\mu g\, m^{-3}$; mean hourly value for 32 days prior to sampling).

Leaf magnetic values (SIRMs), as a proxy for ambient PM_{10} concentrations, can therefore be used to test modelled PM_{10} predictions. Here, we compare the leaf-calculated PM_{10} concentrations around the industrial site with predictions of the contribution from the site's main stack made using a widely used, Gaussian plume air dispersion model, ADMS (CERC, 2010).

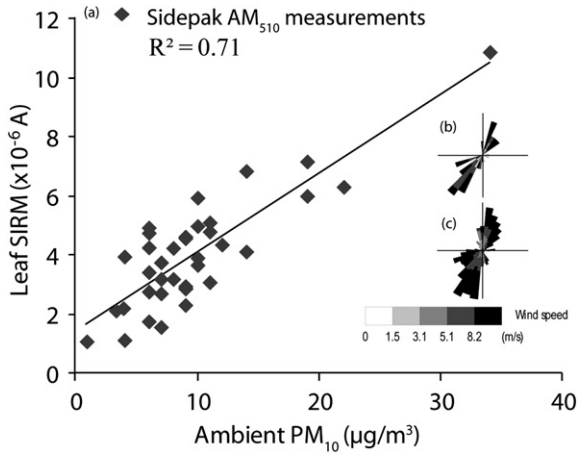

Fig. 4. (a) Correlation of 2009 leaf SIRM values with independently-measured PM_{10} values ($R^2 = 0.71$, $p = 0.01$, $n = 37$.). Local wind speed and direction shown for the 2 days of pumped air sampling (b) 32 days prior to pumped air sampling (c).

The modelled ambient PM_{10} concentrations for the 32 days prior to the September 2009 sampling campaign are shown in Fig. 7b. The maximum peak ($\sim$0.5 μg m^{-3}) occurs $\sim$4 km NNE of the point source stack, with a secondary peak (0.2–0.3 μg m^{-3}) $\sim$4 km SW of the point source stack. Negligible contribution from the plume (<0.02 μg m^{-3}) is modelled within 1 km of the source, and to the NW and SE of the point source. Modelled maximum values occur in the prevailing wind direction (Fig. 6b). This pattern partially corresponds with that indicated by the leaf-calculated PM_{10} values, consistent with a plume 'touch-down' at $\sim$4 km from the source. Locations of modelled and leaf-calculated PM_{10} peak values were similar in the NE quadrant, but differed slightly to the SE and SW (Fig. 7).

However, compared both to the directly-measured and the leaf-calculated PM_{10} concentrations, the modelling (based on stack emissions) under-estimated peak ambient PM_{10} concentrations substantially. The modelled results indicated a maximum stack contribution to ambient PM_{10} concentrations of 0.5 μg m^{-3}. The maximum directly-measured and leaf-derived PM_{10} concentrations were 35 and 42 μg m^{-3}, respectively, at a location within 2 km of the site, and 23 and 27 μg m^{-3}, respectively, at a distance of $\sim$ 4 km from the site, with a background level generally in the 10–15 μg m^{-3} range (Fig. 7a).

4. Discussion

Tree leaves around the industry-influenced area in this study exhibited significant enrichment of their SIRM values, reflecting surface accumulation of particulate pollutants. Maximal leaf SIRM values were consistently observed close to the industrial site (within 2 km radius) and at $\sim$ 4–10 km from the stack in the direction of the prevailing wind (Appendix 2). Absolute (monthly sampling) leaf SIRM values appear to have been affected by both wind velocity and output from the industrial site. In contrast to the evergreen tree species used by Lehndorff et al. (2006), the deciduous leaf-magnetic values measured here display no progressive increase over consecutive monthly samples throughout the in-leaf season. This indicates that the leaf magnetic signature is dominated by particles deposited on the leaf surface (rather than incorporated within the leaf structure). Lower leaf SIRM values were measured in August and September 2008, consistent with a reduction in activity at the industrial site. Additionally, September 2008 was characterised by high levels of rainfall, and low wind speeds (Appendix 2). Higher leaf-SIRMs were measured in June and July 2008, in association with increased activity at the industrial site and in September 2009, consistent with greater wind velocity. ADMS-modelled outputs for the study area indicate particulate deposition from the plume is negligible at wind speeds below 5 m s^{-1}. At higher wind speeds, the plume may lose heat and momentum more quickly, and be 'knocked down' to ground level resulting in raised particulate concentrations (McAlpine and Ruby, 2004).

Table 1
Magnetic properties of samples, indicating maximum and minimum values, with mean and standard deviation.

	Min	Max	Mean	SD
$\%IRM_{20}$	6.39	34.73	15.94	4.41
$\%IRM_{50}$	31.86	66.40	43.41	6.80
$\%IRM_{100}$	40.62	83.74	60.25	6.43
$\%IRM_{300}$	76.35	99.56	93.35	4.25
%HIRM	0.44	24.65	11.81	8.96
$\%HIRM_{af100}$	24.76	52.14	42.15	10.06
χ_{ARM}/SIRM	3.20	101.43	33.85	17.32
MDF_{ARM}	26.06	44.25	37.52	9.78
S ratio	0.65	0.99	0.79	0.05

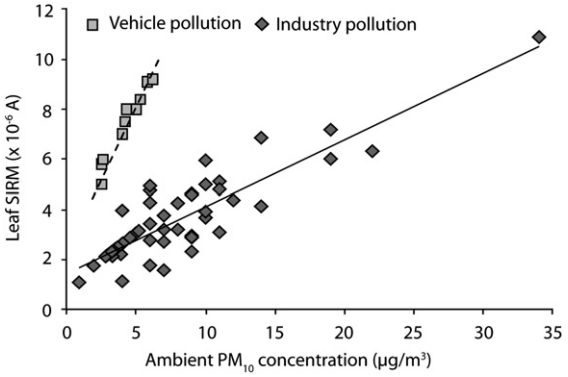

Fig. 5. Correlation of leaf magnetic values and ambient PM_{10} concentrations, derived from vehicle pollution (Hazelrigg UK; high-vol sampling 1636 m^3 collected at a rate of 1133 l/min; Mitchell et al., 2010) and industrial stack point source pollution.

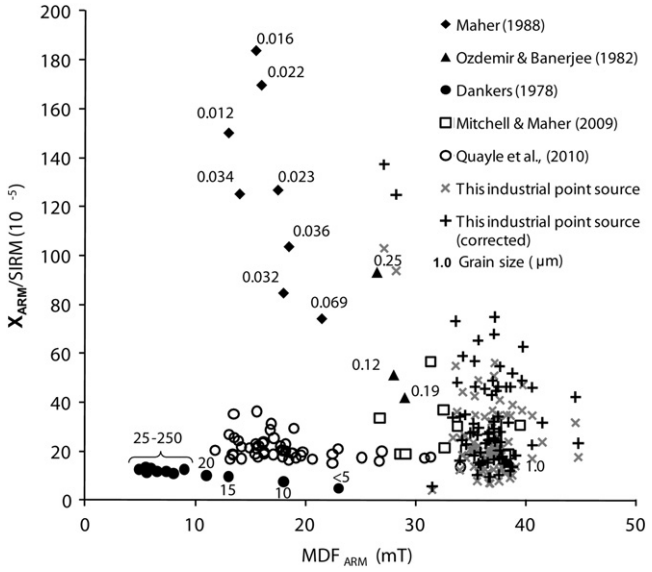

Fig. 6. Comparison of leaf χ_{ARM}/SIRM ratios and MDF_{ARM} values (raw, and corrected for haematite contribution to the SIRM) from around the point source with leaf values from areas with predominantly vehicle- (Mitchell and Maher, 2009) and volcanic-derived particles (Quayle et al., 2010) and magnetite particles of known grain sizes (Maher 1988; Dankers, 1978; Özdemir and Banerjee, 1982).

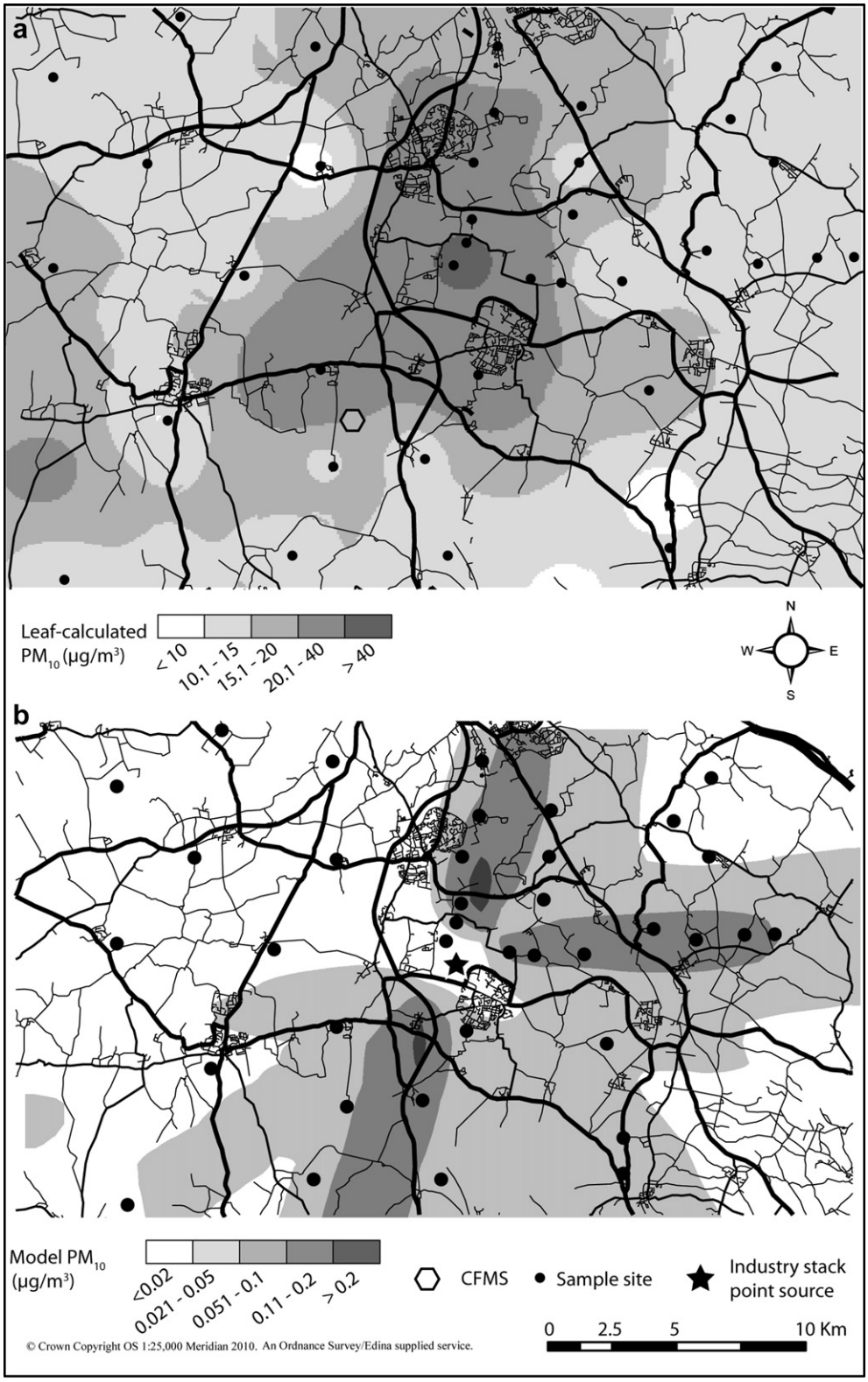

Fig. 7. (a) IDW-interpolated leaf-calculated PM_{10} values and (b) modelled plume based on meteorological conditions for 32 days prior to sampling using standard inputs for source for September (2009).

The spatial patterns of leaf SIRM values correspond with the monthly-averaged prevailing wind direction from the industrial site; they show no correspondence with road networks. The presence of a consistent peak in leaf SIRM values immediately around the combustion plant may reflect fugitive emissions, such as windblown dust from stock piles, conveyor belts and unloading/pulverising of fuel, landfill site activity and/or vehicle movements (trains/heavy goods vehicles/cars) around the site. The lower %

HIRM (<5%) and χ_{ARM}/SIRM ($<13 \times 10^{-5}$ A^{-1}) values of the samples collected within ~ 2 km of the industrial site, compared to more distal samples in the study area, are indicative of a differing mineralogy with a greater concentration of 'softer' magnetic minerals, such as magnetite, of slightly coarser magnetic grain size. Back-calculations using ADMS results indicate that in order to generate the observed near-site PM_{10} concentrations, approximately 5–10 g s^{-1} PM_{10} is required to be generated on site from fugitive sources. Emission factors (U.S. EPA, 2010b) indicate this is a reasonable value, suggesting that fugitive emissions may indeed be contributing to the elevation in local PM_{10} concentrations (i.e. observed within ~2 km of the point source). However, these emissions cannot account for the peaks in PM_{10} concentrations at more distal sample locations.

The data presented here demonstrate that the actively-sampled ambient PM_{10} concentrations and the SIRM values of the passively-collecting leaf samples display a strong direct correlation. As the SidePak AM510 measures at 1 s intervals and returns a mean value over a 5-minute sampling duration, it is susceptible to short-term fluctuations in particle concentration. The manufacturer's reported error for the Sidepak AM_{510} is ±10% but co-location of multiple pumps indicate an error value closer to ±20% at low ambient PM_{10} concentrations (Whyatt, pers comm).

The high level of correlation between the optically-measured PM_{10} concentrations and the leaf SIRM values indicates that the pattern of PM_{10} deposition over the leaf equilibration period was similar to the deposition pattern on the days of active air sampling.

The strong correlation between ambient PM_{10} concentrations and the monthly-integrating leaf SIRM values over this time period demonstrates that leaves provide a representative surface for collection of PM_{10} pollutant particles, and that magnetic measurements of tree leaves provide a robust, quantitative proxy for monthly-averaged ambient PM_{10} particulate concentrations in this single source, industry-dominated setting.

The correlation of leaf SIRM values with ambient PM_{10} concentrations is notably different around this industrial site, compared to a vehicle pollution-influenced area, Hazelrigg, UK (Mitchell et al., 2010). The concentration of haematite was 100 × greater in the particles from the vicinity of the industrial site than those collected at the Hazelrigg roadside.

Magnetite and haematite have both previously been identified in fly ash (e.g. Blaha et al., 2008; Koukouzas et al., 2007), with greater concentrations of haematite than magnetite, particularly where high sulphur fuels/bituminous coals are burned (e.g. Koukouzas et al., 2007). The magnetic fraction of Fe present in fly ash is <50% (McCarthy et al., 1990). In contrast, the magnetic fraction of Fe in vehicle-derived particulate pollution is estimated at ~89% (Maher et al., 2008), predominantly in the form of magnetite (e.g. Abdul-Razzaq and Gautam, 2001; Maher et al., 2008; Mitchell and Maher, 2009). These magnetic contrasts between fly ash and vehicle pollution probably reflect the different stabilities of haematite and magnetite. Both form upon volatilisation and oxidation of Fe-bearing minerals (e.g. pyrite) but at different oxygen concentrations (Hatt and Bull, 1990) and temperatures. In industrial contexts, both magnetite and haematite can form at temperatures exceeding 850 °C, but haematite is stable to higher temperatures (Demir et al., 2001). Vehicle internal combustion engines operate at temperatures < 400 °C (e.g. Einecke et al., 2000) while industrial combustion processes can occur at temperatures exceeding 1100 °C (IEA, 2010).

The strong correlation presented here between leaf SIRM values and ambient PM_{10} concentrations has been obtained in relatively simple situations, with one industrial area in relatively simple topography and in the absence of any transient peaks in long-range transported inputs. Where multiple industrial (or other) activities contribute to the ambient PM_{10} concentrations, the situation is likely to be more complex, due to the differing magnetic signatures of the pollution particles. However, these differences may themselves be used to identify the probable origins of particles contributing to the total ambient burden. Where particles have different sources which are reflected in their magnetic properties, then detailed magnetic analysis can enable 'fingerprinting' and attribution of particulate pollution to specific source types (e.g. Sagnotti et al., 2009; Hansard et al., in preparation). Such source attribution is an essential prerequisite for targeted pollution mitigation.

5. Conclusions

- Measured magnetic properties (SIRMs) of tree leaves represent a robust, quantitative, monthly-averaged proxy for particulate pollution in the vicinity of this industrial source, enabling high-resolution spatial mapping of emission patterns which indicated the likely origins of airborne particles. The leaf-derived PM_{10} concentrations are integrated over ~32 days.
- Samples collected within ~2 km of the industrial site were magnetically distinct from those collected at locations > 2 km from the site. The proximal samples might represent fugitive emissions.
- Correlation between leaf magnetic values and ambient PM_{10} concentrations differs between vehicle- and industry-derived pollution. These differences are likely to arise from differences in particle magnetic composition. Magnetic characterisation of the PM_{10} collected by the leaves indicates that haematite concentrations are ~ 100 × higher in the point source-derived emissions than in the traffic-derived particulate matter.
- The observed differences in the magnetic properties of particulate pollutants emitted from different sources indicate the potential for magnetic source attribution.

Acknowledgements

RH is supported by a NERC (CASE) Studentship award in partnership with the Environment Agency. BAM is supported by a Royal Society Wolfson Research Merit Award. The views presented here are those of the authors and do not necessarily represent those of NERC or the Environment Agency.

AppendixSupplementary data

Supplementary data associated with this article can be found in the online version, at doi:10.1016/j.envpol.2011.02.039.

References

Abdul-Razzaq, W., Gautam, M., 2001. Discovery of magnetite in the exhausted material from the diesel engine. Applied Physics Letters 78, 2018.

Balat, M., 2008. Coal-fired power generation: proven technologies and pollution control systems. Energy Sources, Part A: Recovery, Utilization, and Environmental Effects 30 (2), 132–140.

Blaha, U., Appel, E., Stanjek, H., 2008. Determination of anthropogenic boundary depth in industrially polluted soil and semi-quantification of heavy metal loads using magnetic susceptibility. Environmental Pollution 156, 278–289.

Brook, R., Franklin, B., Cascio, W., Hong, Y., Howard, G., Lipsett, M., Luepker, R., Mittleman, M., Samet, J., Smith, S., Tager, I., 2004. Air pollution and cardiovascular disease: a statement for healthcare professionals from the expert panel on population and prevention science of the American Heart Association. Circulation 109, 2655–2671.

CERC, 2010. ADMS 4. http://www.cerc.co.uk/environmental-software/ADMS-model.html (accessed 18.04.10).

Chamberlain, A., Chadwick, R., 1972. Deposition of spores and other particles on vegetation and soil. Annals of Applied Biology 71 (2), 141–158.

Committee on the Medical Effects of Air Pollutants (COMEAP), 2009. Long-term exposure to air pollution: effect on mortality. http://www.dh.gov.uk/ab/COMEAP/DH_108151 (accessed 07.10.10).
Curtis, L., Rea, W., Smith-Willis, P., Fenyves, E., Pan, Y., 2006. Adverse health effects of outdoor pollutants. Environment International 32, 815–830.
Dankers, P.H., 1978. Magnetic properties of dispersed natural iron oxides of known grain size. PhD Thesis, University of Utrecht.
Demir, I., Hughes, R., DeMaris, P., 2001. Formation and use of coal combustion residues from three types of power plants burning Illinois coals. Fuel 80 (11), 1659–1673.
Einecke, S., Schulz, C., Sick, V., 2000. Measurement of temperature, fuel concentration and equivalence ratio fields using tracer LIF in IC engine combustion. Applied Physics B: Laser and Optics 71, 717–723.
European Environment Agency (EEA), 2008. Emissions of Primary Particles and Secondary Particulate Matter Precursors, CSI 003, Copenhagen.
Frank, U., Nowaczyk, N., 2008. Mineral magnetic properties of artificial samples systematically mixed from haematite and magnetite. Geophysical Journal International 175, 449–461.
Freer-Smith, P., Beckett, K., Taylor, G., 2005. Deposition velocities to Sorbus aria, Acer campestre, Populus deltoides X trichocarpa 'Beaupré', Pinus nigra and X Cupressocyparis Leladii for coarse, fine and ultra-fine particles in the urban environment. Environmental Pollution 133, 157–167.
Hatt, R., Bull, D., 1990. In: Bryers, R.W., Vorres, K.S. (Eds.), Mineral Matter and Ash Deposition from Coal. Engineering Foundation, New York, p. 215.
Halsall, C.J., Maher, B.A., Karloukovski, V.V., Shah, P., Watkins, S.J., 2008. A novel approach to investigating indoor/outdoor pollution links: combined magnetic and PAH measurements. Atmospheric Environment 42, 8902–8909.
Hansard, R., Maher, B.A., Kinnersley, R. Magnetic source attribution for urban atmospheric particulate matter, in preparation.
Hoffmann, V., Knab, M., Appel, E., 1999. Magnetic susceptibility mapping of roadside pollution. Journal of Geochemical Exploration 66 (1–2), 313–326.
IEA Clean coal Centre, 2010. Clean coal technologies: pulverised coal combustion (PCC). http://www.iea-coal.org.uk/site/ieacoal_old/databases/ccts/pulverized-coal-combustion-pcc? (accessed 05.10.10).
Karr, C., Lumley, T., Shepherd, K., Davis, R., Larson, T., Ritz, B., Kaufman, J., 2006. A case–crossover study of wintertime ambient air pollution and infant bronchiolitis. Environmental Health Perspectives 114 (2), 277–281.
Koukouzas, N., Hämäläinen, J., Papanikolaou, D., Tourunen, T., Jäntti, T., 2007. Mineralogical and elemental composition of fly ash from pilot scale fluidised bed combustion of lignite, bituminous coal, wood chips and their blends. Fuel 86, 2186–2219.
Lehndorff, E., Urbat, M., Schwark, L., 2006. Accumulation histories of magnetic particles on pine needles as function of air quality. Atmospheric Environment 40 (36), 7082–7096.
Lu, S.G., Bai, S.Q., 2006. Study on the correlation of magnetic properties and heavy metals content in urban soils of Hangzhou City, China. Journal of Applied Geophysics 60 (1), 1–12.
Maher, B.A., 1988. Magnetic properties of some synthetic sub-micron magnetites. Geophysical Journal 94, 83–96.
Maher, B.A., Karloukovski, V.V., Mutch, T.J., 2004. High-field remanence properties of synthetic and natural submicrometre haematites and goethites: significance for environmental contexts. Earth and Planetary Science Letters 226, 491–505.
Maher, B.A., Moore, C., Matzka, J., 2008. Spatial variation in vehicle-derived metal pollution identified by magnetic and elemental analysis of roadside tree leaves. Atmospheric Environment 42, 364–373.
Maher, B.A., Watkins, S.J., Brunskill, G., Alexander, J., Fielding, C.R., 2009. Sediment provenance in a tropical fluvial and marine context by magnetic 'fingerprinting' of transportable sand fractions. Sedimentology (IF 2.16) 56, 841–861.
Matzka, J., Maher, B.A., 1999. Magnetic biomonitoring of roadside tree leaves: identification of spatial and temporal variations in vehicle-derived particulates. Atmospheric Environment 33, 4565–4569.
McAlpine, J.D., Ruby, M., 2004. Using CFD to Study Air Quality in Urban Microenvironments. In: Zannetti, P. (Ed.), Environmental Sciences and Environmental Computing, vol. II. EnviroComp Institute. http://www.envirocomp.org Chapter 1.
McCarthy, G., Solem, J., Manz, O., Hassett, D., 1990. Use of a database of chemical, mineralogy cal and physical properties of North American fly ash to study the nature of fly ash and it's utilisation as a mineral admixture in concrete. Materials Research Society Symposium Proceedings 178, 3–34.
Minguillón, M., Monfort, E., Querol, X., Alastuey, A., Celades, I., Miró, J., 2009. Effect of ceramic industrial particulate emission control on key components of ambient PM_{10}. Journal of Environmental Management 90 (8), 2558–2567.
Mitchell, R., Maher, B.A., 2009. Evaluation and application of biomagnetic monitoring of traffic-derived particulate pollution. Atmospheric Environment 43, 2095–2103.
Mitchell, R., Maher, B., Kinnersley, R., 2010. Rates of particulate pollution deposition onto leaf surfaces: temporal and inter-species magnetic analyses. Environmental Pollution 158 (5), 1472–1478.
Monn, C., 2001. Exposure assessment of air pollutants: a review on spatial heterogeneity and indoor/outdoor/personal exposure to suspended particulate matter, nitrogen dioxide and ozone. Atmospheric Environment 35 (1), 1–32.
Morris, W.A., Versteeg, J.K., Bryant, D.W., Legzdins, A.E., McCarry, B.E., Marvin, C.H., 1995. Preliminary comparisons between mutagenicity and magnetic- susceptibility of respirable airborne particulate. Atmospheric Environment 29, 3441–3450.
Morton-Bermea, O., Hernandez, E., Martinez-Pichardo, E., Soler-Arechalde, A.M., Lozano Santa-Cruz, R., Gonzalez-Hernandez, G., Beramendi-Orosco, L., Urrutia-Fucugauchi, J., 2009. Mexico City topsoils: heavy metals vs. magnetic susceptibility. Geoderma 151 (3–4), 121–125.
Muxworthy, A.R., Matzka, J., Davila, A.F., Petersen, N., 2003. Magnetic signature of daily sampled urban atmospheric particles. Atmospheric Environment 37, 4163–4169.
Özdemir, Ö., Banerjee, S.K., 1982. A preliminary magnetic study of soil samples from west-central Minnesota. Earth and Planetary Science Letters 59 (2), 393–403.
Parker, S., Kinnersley, R., 2004. A computational and wind tunnel study of particle dry deposition in complex topography. Atmospheric Environment 38 (23), 386.
Pope, C., Ezzati, M., Dockery, D., 2009. Fine-particulate air pollution and life expectancy in the United States. New England Journal of Medicine 360 (4), 376–386.
Quayle, B.M., Mather, T.A., Witt, M.L.I., Maher, B.A., Mitchell, R., Martin, R.S., Calabrese, S., 2010. Application and evaluation of biomagnetic monitoring of volcanically-derived particles at Mt. Etna, Italy. Journal of Volcanology and Geothermal Research 191, 107–116.
Sagnotti, L., Macrí, P., Egli, R., Mondolio, M., 2006. Magnetic properties of atmospheric particulate matter from automatic air sampler stations in Latium (Italy): towards a definition of magnetic fingerprints for natural and anthropogenic PM_{10} sources. Journal of Geophysical Research 111 B12S22.
Sagnotti, L., Taddeucci, J., Winkler, A., Cavallo, A., et al., 2009. Compositional, morphological, and hysteresis characterization of magnetic airborne particulate matter in Rome, Italy. Geochemistry Geophysics Geosystems 10. doi:10.1029/2009GC002563 Q08Z06.
Schwarze, P., Øvrevik, J., Låg, M., Refsnes, M., Nafstad, P., Hetland, R.B., Dybing, E., 2006. Particulate matter properties and health effects: consistency of epidemiological and toxicological studies. Human and Experimental Toxicology 25, 559–579.
Sharma, A., Tripathi, B., 2008. Magnetic mapping of fly-ash pollution and heavy metals from soil samples around a point source in a dry tropical environment. Environmental Monitoring and Assessment 138 (1–3), 31–39.
Szönyi, M., Sagnotti, L., Hirt, A., 2008. A refined biomonitoring study of airborne particulate matter pollution in Rome, with magnetic measurements of Quercus Ilex tree leaves. Geophysical Journal International 173 (1), 127–141.
U.S. EPA, 2010a. AERMOD modelling system. http://www.epa.gov/ttn/scram/dispersion_prefrec.htm#aermod (accessed 12.06.10).
U.S. EPA, 2010b. Emissions factors & AP 42, compilation of air pollutant emission factors. http://www.epa.gov/ttnchie1/ap42/ (accessed 20.09.10).
Wang, F., Chen, D.S., Cheng, S.Y., Li, J.B., Li, M.J., Ren, Z.H., 2010. Identification of regional atmospheric PM_{10} transport pathways using HYSPLIT, MM5-CMAQ and synoptic pressure pattern analysis. Environmental Modelling & Software 25 (8), 927–934.
Woodruff, T.J., Parker, J.D., Schoendorf, K.C., 2006. Fine particulate matter ($PM_{2.5}$) air pollution and selected causes of postneonatal infant mortality in California. Environmental Health Perspectives 114 (5), 786–790.